

Optical Stark decelerator for molecules with a traveling potential wellLianzhong Deng,^{*} Shunyong Hou, and Jianping Yin*State Key Laboratory of Precision Spectroscopy, East China Normal University, Shanghai 200062, People's Republic of China*

(Received 9 December 2016; published 10 March 2017)

We propose a versatile scheme to slow supersonically cooled molecules using a decelerating potential well, obtained by steering a focusing laser beam onto a pair of spinning reflective mirrors under a high-speed brake. The longitudinal motion of molecules in the moving red-detuned light field is analyzed and their corresponding phase-space stability is investigated. Trajectories of CH₄ molecules under the influence of the potential well are simulated using the Monte Carlo method. For instance, with a laser beam of power 20 kW focused onto a spot of waist radius 40–100 μm, corresponding to a peak laser intensity on the order of $\sim 10^8$ W/cm², a CH₄ molecule of ~ 250 m/s can be decelerated to ~ 10 m/s over a distance of a few centimeters on a time scale of hundreds of microseconds.

DOI: [10.1103/PhysRevA.95.033409](https://doi.org/10.1103/PhysRevA.95.033409)**I. INTRODUCTION**

Manipulation of both the internal and external degrees of freedom of neutral molecules in the gas phase has been a hot subject in atomic and molecular physics for decades. Over the past years, a number of techniques and schemes have been proposed or demonstrated to slow the motion of supersonically cooled neutral molecules of chemical stability, such as the electrostatic Stark decelerator [1–9], the Zeeman decelerator [10–15], and the optical Stark decelerator [16–21]. Big successes have been made on either the electrostatic Stark decelerator or the Zeeman decelerator and molecules can be precisely brought to any desired velocity. For the optical Stark decelerator, however, this kind of precise control on molecule velocity has not been achieved yet.

In 2004, Fulton *et al.* first demonstrated decelerating molecules with a single laser pulse of duration ~ 15 ns [19]. A maximum reduction of ~ 25 m/s in molecule velocity was observed with a peak laser intensity of 1.6×10^{12} W/cm², corresponding to a potential well depth of 253 K. Later, they reported an experimental study on controlling the motion of molecules with pulsed optical lattices of 5.8 ns in duration [20]. The kinetic energy of the molecules was reduced by up to 50% with an intense laser field of 10^{11} W/cm², corresponding to a potential well depth of 22 K. However, the short time duration and lack of mobility of the potential well prevents it from being fully used in slowing the molecules in both experiments. Another way to optically decelerate molecules is using moderate laser intensities but with longer time duration. A traveling potential well will then be needed to effectively decelerate the molecules of high kinetic energy, since the well depth is rather shallow now. Otherwise, the molecules will escape from the potential well soon. Early in 2000, Friedrich [16] proposed scooping molecules at right angles by a nonresonant laser beam decelerated on a circular path. A strong centripetal force is required in order for the scooped molecules to follow the circular motion of the laser beam focus. For instance, a molecule of ~ 250 m/s orbiting around a circular path of ~ 1 m in radius needs a centripetal

acceleration of about $\sim 6.25 \times 10^4$ m/s². However, such a strong force is not available along the direction of the laser propagation.

In this paper, we propose a versatile method to decelerate supersonically cooled atoms or molecules using a traveling potential well, which is formed by steering a focusing laser beam onto a pair of spinning reflective mirrors under a high-speed brake. The schematic diagram and operation principle of the method are first presented. The longitudinal motion of slowing molecules and their corresponding phase-space stability are then investigated. Trajectory simulations of CH₄ molecules moving in the decelerating potential well are performed using the Monte Carlo method, which is followed by some analysis and discussion. A conclusion is given at the end.

We show interest in the methane (CH₄) molecule here for a couple of reasons. Firstly, it is taken as a representative of nonpolar molecules and can be efficiently decelerated using a laser field due to its large ratio of electric polarizability to mass. Currently, polar (or paramagnetic) molecules can be effectively decelerated by using other well-developed techniques, such as the electrical Stark decelerator (or the Zeeman decelerator). For molecules with neither electric nor magnetic dipole moment, the optical Stark decelerator is a choice. Secondly, the long interaction time of decelerated or trapped methane with light or other material particles can help us not only better understand its physical and chemical properties but also offer important applications, such as high-resolution Doppler-free spectroscopy for optical frequency standards [22] or molecular clocks [23]. Thirdly, methane is the simplest alkane and is the main constituent of natural gas. The relative abundance of methane on earth makes it an attractive fuel. Methane has been detected or is believed to exist on all planets of the solar system and interstellar clouds. Methane has also been proposed as a possible rocket propellant on future space missions, especially for interstellar traveling. But capturing and storing it poses challenges, especially when it is in a low-density gaseous state. Studies on interactions of decelerated (cold) methane with other (gaseous, liquid, or even solid) material might help in capturing, condensing, and storing gaseous methane *in situ* for rocket fuel in the future in outer space, where both the local temperature and gas density might be rather low.

^{*}lzdeng@phy.ecnu.edu.cn

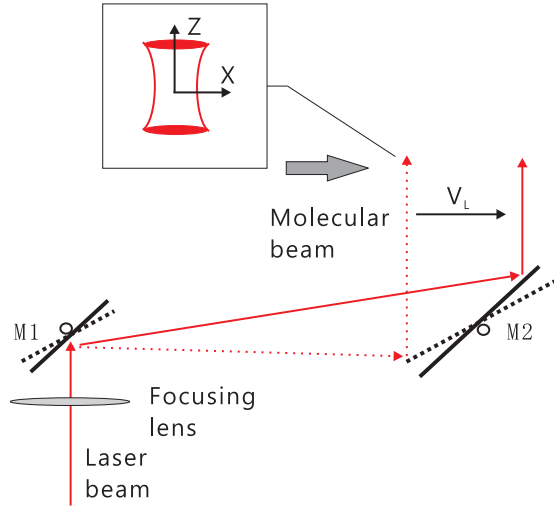


FIG. 1. Schematic diagram for decelerating molecular beams using a traveling light field.

II. SCHEME AND SLOWING PRINCIPLE

A. Scheme of the versatile optical Stark decelerator

The schematic diagram of our proposed optical Stark decelerator is plotted in Fig. 1. A laser beam is reflected consecutively by two mirrors M1 and M2 in parallel. The laser beam is focused to form an intense light field at the spot, as shown by the inset. When the mirrors M1 and M2 spin simultaneously, a moving laser spot is obtained in the direction perpendicular to the laser beam axis, i.e., the X direction, as shown in Fig. 1. A supersonically cooled molecular beam moving in direction X has its central section overlapped in space with the traveling laser spot. The spot serves as an optical trap for the molecules when the laser frequency is far-red detuned. When the spinning mirrors M1 and M2 are under a simultaneous brake, the traveling optical potential well will be decelerated, and so will the molecules trapped by it. The final speed of the trapped molecules depends upon that of the traveling potential well.

B. Longitudinal motion and phase-space stability

The red-detuned light field is assumed to have a Gaussian intensity distribution in the longitudinal (i.e., X) direction. The corresponding dipole potential energy for a molecule at position X is given by

$$W = -(1/2)\alpha |E(X)|^2 = -(\alpha I_0/\varepsilon_0 C) \exp[-2(X/w)^2], \quad (1)$$

where I_0 is the maximum laser intensity at $X = 0$, α is the averaged molecular polarizability, ε_0 is the permittivity in free space, and w is the waist radius of the focused laser spot. The corresponding dipole force per unit mass in the X direction is given by

$$\beta = -\nabla W_X/m = -C_0 X \exp[-2(X/w)^2], \quad (2)$$

where $C_0 = 4\alpha I_0/m\varepsilon_0 C w^2$ and m is the mass of the molecule. A brief examination of Eq. (2) indicates that the maximum

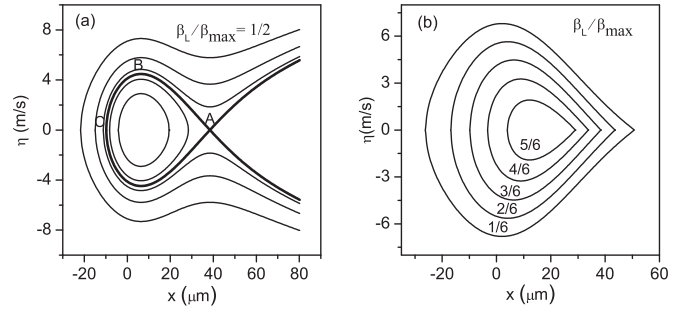


FIG. 2. (a) The trajectories of both trapped and untrapped CH_4 molecules in the phase space with $\beta_L = \beta_{\max}/2$. (b) The phase stable areas for CH_4 molecules in the decelerating potential well with $\beta_L/\beta_{\max} = 1/6, 2/6, 3/6, 4/6$, and $5/6$, respectively.

value of β is obtained at $X = w/2$, and one has

$$\beta_{\max} = C_0 w / (2\sqrt{e}). \quad (3)$$

When the potential well is decelerating at a constant rate of β_L in the X direction, the equation of motion for molecules is given by

$$\ddot{x} = -C_0(X - v_0 t + \beta_L t^2/2) \times \exp[-2(X - v_0 t + \beta_L t^2/2)^2/w^2], \quad (4)$$

where v_0 is the initial velocity of the decelerating potential well. We introduce a quantity of the relative position x , defined as $x = X - v_0 t + \beta_L t^2/2$, corresponding to the molecule position with respect to the center of the decelerating potential well. Similarly, a quantity of the relative velocity η , defined as $\eta = dx/dt$, can be introduced. Thus, in the reference frame fixed on the decelerating potential well, the equation of motion for molecules is given by

$$\dot{x} = d\eta/dt = -C_0 x \exp[-2x^2/w^2] + \beta_L. \quad (5)$$

By integration of Eq. (5), we have

$$\eta^2 = (C_0 w^2/2) \exp(-2x^2/w^2) + 2\beta_L x + C_{\text{Integ}}, \quad (6)$$

with C_{Integ} being an integration constant. Equation (6) describes the trajectories of molecules in the phase space $[x, \eta]$ under the interaction with the decelerating potential well. By solving the differential equation, $d(\eta^2)/dx = 0$, and using Eq. (6), one can determine the value of C_{Integ} for a possible phase stable area. Molecules accepted by this area will be trapped and simultaneously decelerated.

Let us take the methane molecule (CH_4 , $\alpha \approx 2.9 \times 10^{-40} \text{ C m}^2 \text{ V}^{-1}$) for an example. With a laser power of 20 kW and a focused beam waist radius of $w = 40 \mu\text{m}$, corresponding to a peak laser intensity of $I_0 \approx 8.0 \times 10^8 \text{ W/cm}^2$, the maximum value of β (i.e., β_{\max}) available for the molecules is about $\sim 9.91 \times 10^5 \text{ m/s}^2$. As we shall see later, the deceleration rate of the potential well being used, β_L , should never be more than β_{\max} for a stable decelerator. Figure 2(a) shows the motional trajectories of both trapped and untrapped methane molecules in phase space with $\beta_L = \beta_{\max}/2$. The middle closed, thick curve indicates the separatrix of a stable region in phase space with three critical points A, B, and C being marked. A molecule moving along this trajectory has its maximum velocity (i.e., $\eta = \eta_{\max}$) at point B, and is gradually

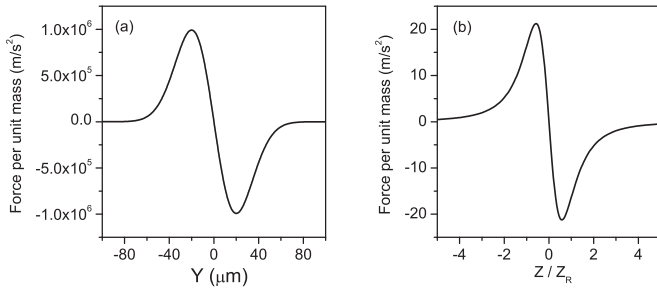


FIG. 3. The force per unit mass experienced by the CH_4 molecule as a function of displacement from the focus center along the Y direction (a) and Z direction (b).

slowed when moving forward toward point A. The molecule has its velocity reduced to zero (i.e., $\eta = 0$) at point A. If the molecule turns back successfully at point A, it will move backward along the lower part of the trajectory. The molecule will be accelerated and then decelerated before it arrives at point C. When its velocity reduces to zero again at point C, the molecule will be turned back and accelerated toward point B. Molecules initially accepted by this area can oscillate stably in the potential well and be decelerated. Molecules initially outside this region, however, cannot undergo stable deceleration though their velocities might be perturbed by the potential well.

The size of the phase stable area depends on the deceleration rate β_L of the potential well in a way much similar to that of a conventional electrostatic Stark decelerator [2]. The phase stable area has its maximum size obtained at $\beta_L = 0$ and decreases with increasing value of β_L . It reduces to zero as $\beta_L = \beta_{\max}$. A phase stable area of finite size exists for $0 < \beta_L < \beta_{\max}$. Figure 2(b) shows the separatrices of the phase stable areas with $\beta_L/\beta_{\max} = 1/6, 2/6, 3/6, 4/6$, and $5/6$, respectively. The maximum values of η , η_{\max} that still can be accepted by the phase stable area are about 6.8, 5.6, 4.5, 3.3, and 1.9 m/s, respectively. Generally, a larger value of β_L corresponds to a stronger deceleration, and the potential well can be decelerated to a target velocity over a shorter distance within a shorter time, while a smaller value of β_L means a bigger phase-space area, and more molecules can be accepted and decelerated by the potential well. Therefore there is a compromise in selecting β_L in practice.

C. Transverse confinement

For a Gaussian laser beam of cylindrical symmetry, the light field is identical in the two directions (i.e., directions X and Y) perpendicular to its beam axis (direction Z). Therefore, the motion of molecules in the Y direction is governed by the same Eqs. (5) and (6) but with $\beta_L = 0$. Figure 3(a) shows the force per unit mass (or acceleration) experienced by the CH_4 molecule along direction Y in the optical trap. The maximal acceleration is $\sim 9.91 \times 10^5 \text{ m/s}^2$, the same as that in direction X . Figure 3(b) shows the force per unit mass for the CH_4 molecule along the laser beam axis as a function of Z/Z_R . Here $Z_R = \pi w^2/\lambda$ is the Rayleigh length of the laser focus spot and λ is the laser wavelength ($\sim 1.064 \mu\text{m}$). The effective length of the focus spot can be characterized by two times

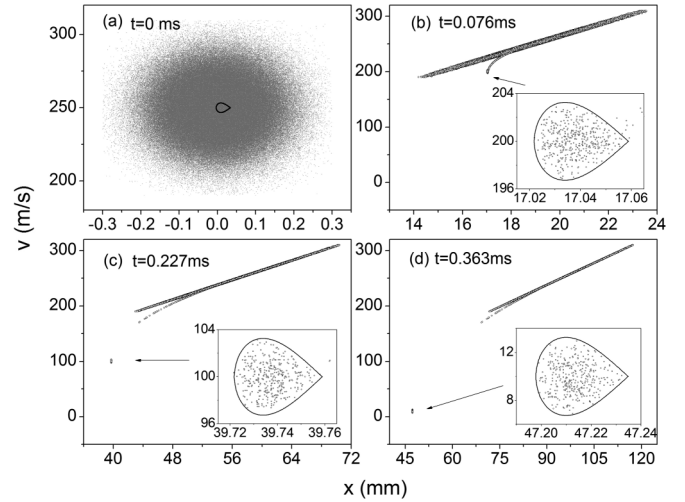


FIG. 4. The distribution of the molecular pulse in phase space at time $t = 0 \text{ ms}$ (a), 0.076 ms (b), 0.227 ms (c), and 0.363 ms (d) with $\beta_L = \beta_{\max}/3$ (simulation results). The insets show a closeup of the phase-space distribution of the molecular packet (indicated by arrows) decelerated along with the potential well.

Z_R . The maximal acceleration in direction Z is just about $\sim 21.20 \text{ m/s}^2$ and far less than those in both directions X and Y . Therefore, the confinement of molecules in the Z direction is rather weak and can be neglected. So the potential well in our scheme is actually a 2D trap for molecules, similar to that studied by Fulton *et al.* [19].

D. Numeric simulation

Trajectories of CH_4 molecules with the presence of the decelerating potential well are simulated using Monte Carlo method to testify our proposed scheme. The pulsed CH_4 molecular beam has a translational temperature of 2 K with its most probable velocity of $v = 250 \text{ m/s}$ along direction X , which is the same as the initial velocity of the potential well. The molecular beam has its transverse velocity centered at zero with a full width at half maximum (FWHM) spread of $\sim 10 \text{ m/s}$ for both directions Y and Z . Figure 4 shows the time evolution of the molecular pulse in phase space with $\beta_L = \beta_{\max}/3 = 6.60 \times 10^5 \text{ m/s}^2$. The potential well is assumed to overlap with the central section of the molecular pulse at $t = 0 \text{ ms}$, as shown in Fig. 4(a). Each gray dot corresponds to a molecule in the phase space $[v, x]$. The solid line indicates the separatrix of the phase stable area calculated from Eq. (6) with $\beta_L = \beta_{\max}/3$. Figures 4(b)–4(d) show the phase-space distribution of the molecular pulse in the longitudinal direction at time points of $t \approx 0.076$, ~ 0.227 , and $\sim 0.363 \text{ ms}$, respectively. The insets zoom in on the phase-space distribution of the molecular packet (indicated by arrows) decelerated along with the potential well, and simulated results fall perfectly within the separatrix (solid line) of the phase stable area derived from Eq. (6). The instantaneous velocities of the potential well are ~ 200 , ~ 100 , and $\sim 10 \text{ m/s}$ at three time points, and the distances that the well traveled are about ~ 1.703 , ~ 3.973 , and $\sim 4.721 \text{ cm}$, respectively, as can be found in the insets.

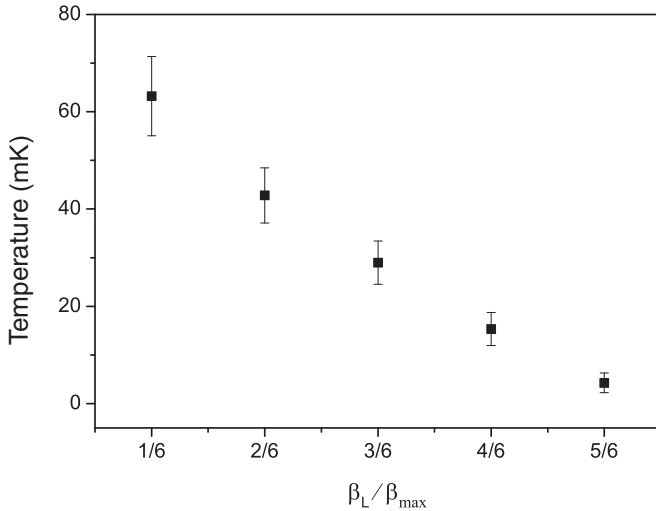


FIG. 5. Temperatures of the decelerated molecular packets as a function of β_L .

The results clearly show that molecules initially accepted by the phase stable area can be stably decelerated with the potential well and keep their phase-space density invariant, as shown by the insets. Some molecules initially near the separatrix of the phase stable area have their velocities affected but finally escape from the potential well, as shown by the tiny branch in Figs. 4(b)–4(d). Most molecules are hardly affected by the decelerating well and remain at their original velocities; they form the majority of the molecular pulse profile in phase space. A real pulsed molecular beam usually lasts tens of microseconds in time and thus extends a few millimeters or even longer in space. For our proposed scheme here, the size of the optical trap is on the order of tens of micrometers along the molecular beam axis. Only a tiny portion of the molecular beam overlapping the laser focus can be captured by the optical trap. During our simulation, the pulsed molecular beam is chosen to be short so that the total number of molecules does not exceed the dynamic memory of our PC and the total computation time is within tolerance, but long enough so that the physical process being explored can still be well manifested without loss of fidelity.

Trajectory simulations of CH_4 molecules are also performed for different values of β_L and similar results are obtained. For each case, molecules in the decelerated molecular packet are statistically counted and their velocity distribution is examined. The translational temperature of the decelerated molecular packet, T_{Tr} , is defined as $K T_{Tr} = m \Delta v_X^2 / 2$. Here K is the Boltzmann constant, m is the mass of the molecule, and Δv_X is the FWHM velocity spread of the decelerated packet in the longitudinal direction of X . For each case of β_L , Δv_X is obtained by Gaussian fitting the corresponding velocity distribution of the molecular packet. The respective values of T_{Tr} are ~ 63 , ~ 42 , ~ 29 , ~ 15 , and ~ 4 mK for $\beta_L/\beta_{\max} = 1/6, 2/6, 3/6, 4/6$, and $5/6$, as shown by solid squares in Fig. 5. As expected, the temperature of the slowed molecular packet is decreased with the increase of the deceleration rate β_L . The temperature T_{Tr} is also an indication of the depth of the potential well.

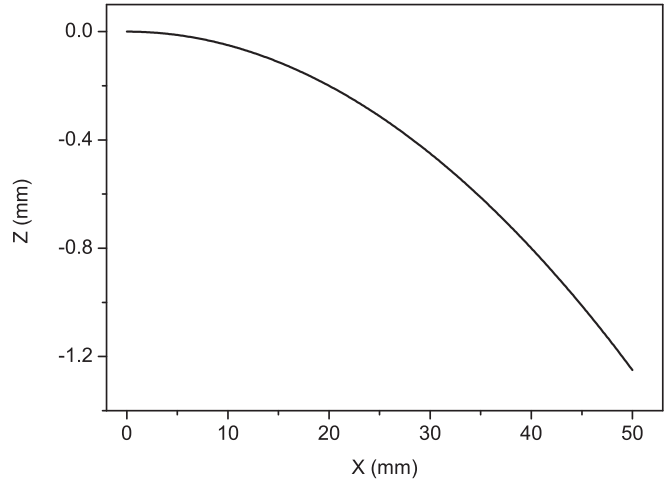


FIG. 6. The relationship between the X position and Z position of the laser focus center. The distance between mirrors M1 and M2 is taken as 1 m.

III. ANALYSIS AND DISCUSSION

One problem concerning our scheme is the shift of the focus spot in space as the laser is moving along the molecular beam axis. The focus center of the laser beam does not move perfectly in a straight line but moves slightly closer to mirror 2 when the optical trap is being decelerated along the direction of X . Figure 6 shows the relationship between the X position and Z position of the laser focus center. The distance between mirror M1 and M2 is taken as 1 m. For instance, when the optical trap is decelerated over a distance of 50 mm along the X direction, the focus center shifts slightly about ~ 1.25 mm toward mirror 2 in the Z direction. For a Gaussian laser beam the effective length of the focus spot can be characterized by two times the Rayleigh length, $2Z_R = 2\pi w^2/\lambda$. For instance, a focusing beam of $w = 40 \mu\text{m}$ in waist radius and $\lambda = 1.064 \mu\text{m}$ in wavelength has an effective focus spot of $2Z_R = 9.44$ mm in length, which is much larger than the focus shift of ~ 1.25 mm. One may ignore the influence of the focus shift so long as it is much less than the effective length of the spot.

Another problem concerns the feasibility of controlling the spinning mirrors M1 and M2. If M2 is placed 1 m away from M1, the mirrors will need to spin at a frequency of about 20 Hz (i.e., 1200 rpm) to produce a translational velocity of $v_L = 250$ m/s for the potential well moving along the molecular beam axis. For a selected deceleration rate of $\beta_L = \beta_{\max} 2/3 = 6.60 \times 10^5 \text{ m/s}^2$, it will take about ~ 0.363 ms to bring the potential well of 250 m/s to a velocity of ~ 10 m/s over a distance of about ~ 4.721 cm. The control of the rotating mirror has a strong dependence on its moment of inertia, I . To reduce the value of I for better control one can design the shape of the mirror as follows: a cubic glass bar mirror of 10 mm in width, 10 mm in height, and 50 mm in length. The mass of the bar is calculated to be about 12.5 g for an assumed glass density of 2.5 g/cm^3 . The moment of inertia is estimated to be about $\sim 2.0 \times 10^{-6} \text{ kg m}^2$ when the bar mirror rotates about its center of mass. A torque of 0.66 N m is required in theory to produce an angular acceleration of $\sim 3.30 \times 10^5 \text{ rad/s}^2$ and thus

a linear tangential acceleration of $\beta_L = 6.60 \times 10^5 \text{ m/s}^2$. The requirements in both angular rotation speed ($\sim 1200 \text{ rpm}$) and torque ($\sim 0.66 \text{ N m}$) are of no challenge to the current motor technology and might even be met directly by commercial products [24] with little modification. The moment of inertia of the glass bar may be further reduced if it is gradually tapered in size toward both of its ends, similar to the design of a rotating supersonic nozzle for producing slow molecules [25]. An alternative design might be a full-metal bar mirror (hollow inside) of the same size.

If a smaller acceleration is available due to some kind of practical limitation, the molecules can still be effectively decelerated. The final velocity of the molecular packet is governed by the product of β_L and t as $v_f = v_0 - \beta_L t$, with v_0 being the initial velocity and t the interaction time of light and molecules. In the experiments of Fulton *et al.*, very big values of deceleration rate ($10^8 - 10^9 \text{ m/s}^2$) and very short interaction times of t ($\sim 10 \text{ ns}$) were used to slow molecules [19,20]. In our proposed scheme here only moderate values of deceleration rate ($10^5 - 10^6 \text{ m/s}^2$) are considered. This weakness in the deceleration rate is, however, compensated for by a long interaction time of t (on the order of a submillisecond). This lengthening in time is, in theory, expected to offer better control on the velocity of the molecular packet. In fact, β_L need not be constant and can fluctuate during the deceleration process so long as it is less than the maximum deceleration of the optical field β_{max} and guarantees a phase stable region of finite size always present for the decelerating molecules; and the final velocity of the molecular packet depends solely on the rotation speed of the stalling mirror the moment the laser leaves its reflective surface.

For the CH_4 molecules studied here, a laser beam of power 20 kW focused onto a spot of waist radius 40–100 μm can offer a deceleration rate of $10^5 - 10^6 \text{ m/s}^2$. Surely, the more intense the light field is, the deeper the optical trap for the molecules will be. With the advancement of laser technology single-mode cw lasers of power up to $\sim 20 \text{ kW}$ and multimode cw lasers of power up to $\sim 500 \text{ kW}$ are now commercially available [26].

The total number N of molecules accepted by the potential trap can be estimated as $N = fnV$ [16]. Here, n is the number density of molecules. V is the effective volume of the trap, out of which the laser intensity decreases to below half the maximum value, estimated as $V = w^2 2(Z_R) = 2\pi w^4/\lambda$ with w the laser beam waist and λ the laser wavelength. f is the fraction of molecules whose velocities fall in the range of

$[v_0 - \eta_{\text{max}}, v_0 + \eta_{\text{max}}]$ with η_{max} being the maximum velocity accepted by the trap. For a laser focus spot of waist radius 40–100 μm , the effective volume of the trap V is on the order of 10^{-5} cm^3 ($\lambda = 1.064 \mu\text{m}$). Suppose the supersonic CH_4 molecular beam has a translational temperature of $\sim 2 \text{ K}$ with number densities of $10^{13} - 10^{14} \text{ molecules/cm}^3$ [16]. For the studied case of $\eta_{\text{max}} = 3.3 \text{ m/s}$ (i.e., $\beta_L = 2\beta_{\text{max}}/3 = 6.60 \times 10^5 \text{ m/s}^2$) above, the total number of molecules captured by the optical trap is on the order of $10^6 - 10^7$.

IV. CONCLUSION

In this paper, we have proposed a versatile scheme to slow supersonically cooled molecules using a decelerating optical potential well, obtained by steering a focused laser beam onto a pair of spinning reflective mirrors under a high-speed brake. The traveling potential well causes the interaction between molecules and the light field to be maintained for a relatively long time over a long distance. The weak slowing effect of the molecules thus accumulates and they are effectively decelerated. We analyzed the longitudinal motion of molecules in the moving potential well and investigated their corresponding phase-space stability as a function of deceleration rate. Trajectories of CH_4 molecules under the influence of the potential well were numerically simulated and the behavior of the decelerated molecular packet agreed well with that analytically predicted. The velocity of the captured molecular packet can be brought to any desired value, depending upon the speed of the potential well. For instance, a laser beam of power 20 kW focused onto a spot of waist radius 40–100 μm can offer a deceleration rate of $10^5 - 10^6 \text{ m/s}^2$ and a CH_4 molecule of $\sim 250 \text{ m/s}$ can be brought to $\sim 10 \text{ m/s}$ over a length of a few centimeters on a time scale of hundreds of microseconds. The total number of molecules captured by the optical trap is on the order of $10^6 - 10^7$ for supersonic CH_4 molecular beams having densities of $10^{13} - 10^{14} \text{ molecules/cm}^3$. Our proposed scheme is versatile and can be used to decelerate, guide, and accelerate molecules; it all depends on how one controls the rotating mirrors. The proposed scheme is applicable to manipulation of atoms as well.

ACKNOWLEDGMENT

We acknowledge financial support from the National Nature Science Foundation of China (NSFC) (Grants No. 11504112, No. 91536218, and No. 11604100).

-
- [1] H. L. Bethlem, G. Berden, and G. Meijer, *Phys. Rev. Lett.* **83**, 1558 (1999).
 - [2] H. L. Bethlem, F. M. H. Crompvoets, R. T. Jongma, S. Y. T. van de Meerakker, and G. Meijer, *Phys. Rev. A* **65**, 053416 (2002).
 - [3] J. R. Bochinski, E. R. Hudson, H. J. Lewandowski, G. Meijer, and J. Ye, *Phys. Rev. Lett.* **91**, 243001 (2003).
 - [4] M. R. Tarbutt, H. L. Bethlem, J. J. Hudson, V. L. Ryabov, V. A. Ryzhov, B. E. Sauer, G. Meijer, and E. A. Hinds, *Phys. Rev. Lett.* **92**, 173002 (2004).
 - [5] E. R. Hudson, C. Ticknor, B. C. Sawyer, C. A. Taatjes, H. J. Lewandowski, J. R. Bochinski, J. L. Bohn, and J. Ye, *Phys. Rev. A* **73**, 063404 (2006).
 - [6] S. Jung, E. Tiemann, and Ch. Lisdat, *Phys. Rev. A* **74**, 040701 (2006).
 - [7] S. A. Meek, H. L. Bethlem, H. Conrad, and G. Meijer, *Phys. Rev. Lett.* **100**, 153003 (2008).
 - [8] M. Quintero-Pérez, P. Jansen, T. E. Wall, J. E. van den Berg, S. Hoekstra, and H. L. Bethlem, *Phys. Rev. Lett.* **110**, 133003 (2013).

- [9] S. Hou, S. Li, L. Deng, and J. Yin, *J. Phys. B* **46**, 045301 (2013).
- [10] N. Vanhaecke, U. Meier, M. Andrist, B. H. Meier, and F. Merkt, *Phys. Rev. A* **75**, 031402 (2007).
- [11] S. D. Hogan, A. W. Wiederkehr, H. Schmutz, and F. Merkt, *Phys. Rev. Lett.* **101**, 143001 (2008).
- [12] E. Narevicius, A. Libson, C. G. Parthey, I. Chavez, J. Narevicius, U. Even, and M. G. Raizen, *Phys. Rev. Lett.* **100**, 093003 (2008).
- [13] E. Narevicius, A. Libson, C. G. Parthey, I. Chavez, J. Narevicius, U. Even, and M. G. Raizen, *Phys. Rev. A* **77**, 051401 (2008).
- [14] A.W. Wiederkehr, H. Schmutz, and F. Merkt, *Mol. Phys.* **110**, 1807 (2012).
- [15] M. Motsch, P. Jansen, J. A. Agner, H. Schmutz, and F. Merkt, *Phys. Rev. A* **89**, 043420 (2014).
- [16] B. Friedrich, *Phys. Rev. A* **61**, 025403 (2000).
- [17] P. F. Barker and M. N. Shneider, *Phys. Rev. A* **64**, 033408 (2001).
- [18] G. Dong, W. Lu, and P. F. Barker, *Phys. Rev. A* **69**, 013409 (2004).
- [19] R. Fulton, A. I. Bishop, and P. F. Barker, *Phys. Rev. Lett.* **93**, 243004 (2004).
- [20] R. Fulton, A. I. Bishop, M. N. Shneider, and P. F. Barker, *Nat. Phys.* **2**, 465 (2006).
- [21] Y. Yin, Q. Zhou, L. Deng, Y. Xia, and J. Yin, *Opt. Express* **17**, 10706 (2009).
- [22] B. Bodermann, M. Klug, H. Knöckel, E. Tiemann, T. Trebst, and H. R. Telle, *Appl. Phys. B* **67**, 95 (1998).
- [23] S. M. Foreman, A. Marian, J. Ye, E. A. Petrukhin, M. A. Gubin, O. D. Mücke, F. N. C. Wong, E. P. Ippen, and F. X. Kärtner, *Opt. Lett.* **30**, 570 (2005).
- [24] <http://www.maxonmotor.com.au/maxon/view/category/>.
- [25] L. Sheffield, M. Hickey, V. Krasovitskiy, K. D. D. Rathnayaka, I. F. Lyuksyutov, and D. R. Herschbach, *Rev. Sci. Instrum.* **83**, 064102 (2012).
- [26] http://www.ipgphotonics.com/group/view/8/Lasers%2FHigh_Power_CW_Fiber_Lasers.